A Comprehensive p53 Drug Discovery Platform: From Target-Based Assays to In Vivo Models

Aicheng Wang, Kejun Mao, Tao Li, Lizhao Guan, Dongfeng He, Haiting Dai, Haichao Wang, Chunling Li, Cong Huang, and Tiejun Bing;
International Division, ICE Bioscience Inc., Beijing, China

ICE Innovative CRO+Explorer ICE Bioscience

Introduction

The study of the TP53 gene, commonly referred to as p53, holds paramount importance in the field of cancer research and the DNA Damage Response (DDR). p53 is regarded as one of the most pivotal tumor suppressor genes due to its role in safeguarding genomic integrity and orchestrating DDR mechanisms. It plays a multifaceted role in maintaining cellular homeostasis by coordinating processes such as DNA repair, cell cycle regulation, and apoptosis, all of which are vital components of the DDR. Understanding p53 and its functions has become essential for devising targeted therapies and novel drug development in the fight against cancer while also shedding light on DDR mechanisms.

The TP53 Y220C mutation, among others, has emerged as a major challenge in p53-related research and drug development. This mutation results in the loss of p53's ability to effectively regulate gene repair mechanisms and apoptosis, both of which are critical components of DDR. Consequently, it promotes the development and progression of tumors, rendering the mutant p53 an attractive target for therapeutic interventions. However, the complexity of various p53 mutations poses a formidable obstacle in drug design and development, necessitating innovative approaches to address this issue.

To address the challenges, we have established a dedicated p53-based research platform that encompasses a wide array of ready-to-use assays, both in vitro and in vivo. Our platform begins with the purification and expression of p53 proteins and extends to biochemical assays, cell line engineering, cellular phenotypic assays, animal models, and in vivo pharmacology studies. This platform serves to bridge existing gaps in the current research landscape, facilitating more efficient and effective investigations into p53-related therapeutics and their role in DDR.

Methods

- P53/DNA Interaction Assay: Mixed 40μL of compound, enzyme, and Biotin-BIM substrate with MAb-Anti-His-Tb & SA-d2. Incubated 70 mins at RT; signal measured with BMG Labtech.
- Cell Proliferation Assay: Medium and CellTiter-Glo reagent mixed 1:1. Incubated 30 mins at RT; fluorescence measured with BMG Labtech.
- Bright-Lite Luciferase Assay: Medium combined with Bright-Lite reagent 2:1. Incubated 3 mins at RT; fluorescence detected with BMG Labtech.
- GSH Assay: Cells harvested and processed with standard reagents. Analysis performed using BMG Labtech.

P53 Recombinant Proteins

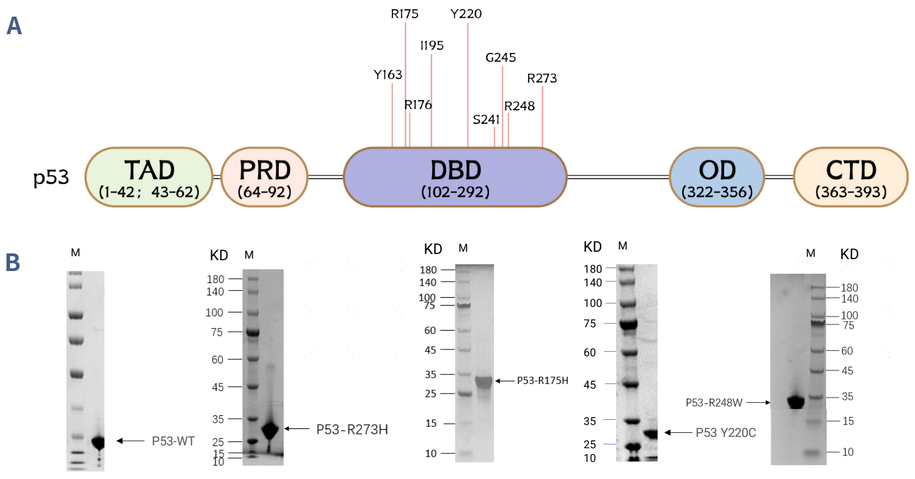

Figure 3. (A) P53 protein and regions. (B) P53 and its mutant proteins. Wild Type p53 WT and (B-E) mutant p53 R273H, p53 R175H, p53 Y220C, p53 R248W proteins. Partial recombinant proteins are available at ICE Bioscience.

Biochemical Assays for p53

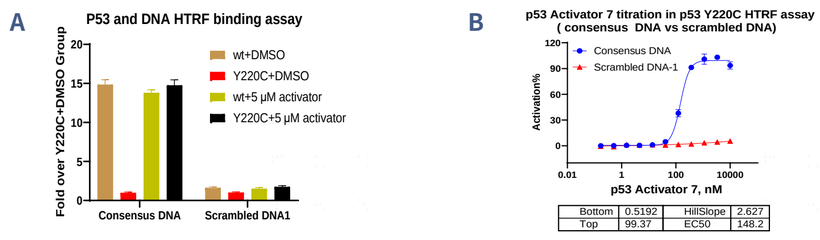

Bottom	0.5192	HillSlope	2.627
Top	99.37	EC50	148.2

Figure 4. Detection of p53 and DNA interaction based on HTRF.

(A) The interaction between p53 WT (wild-type) and consensus DNA was notably observed, whereas p53 Y220C did not exhibit such interaction. However, the binding between p53 Y220C and consensus DNA could be restored when an activator, which had no effect on p53 WT, was introduced. As a control, scrambled DNA was included, and neither p53 WT nor p53 Y220C exhibited interaction to scrambled DNA, regardless of the presence of the activator.

(B) The compound p53 activator 7, a reference compound, effectively enhanced the interaction between p53 Y220C and consensus DNA, with an EC50 of approximately 150 nM. Notably, the interaction between p53 Y220C and scrambled DNA remained undetectable.

Cell Proliferation Assay

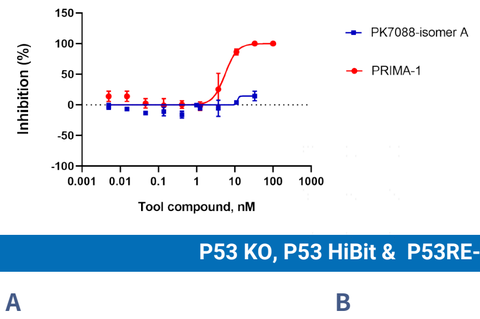

	PK7088-isomer A	PRIMA-1
IC50	>30	5.853

Figure 5. Figure: Dose-dependent effects of PK7088-isomer A and PRIMA-1 on cell proliferation in Huh7 cell lines. PRIMA-1 is a small molecule known to restore the tumor suppressor function of mutant p53, with a potential role in cancer therapy by inducing apoptosis and inhibiting tumor growth.

P53 KO, P53 HiBit & P53RE-Luc2P Cell Line Generation

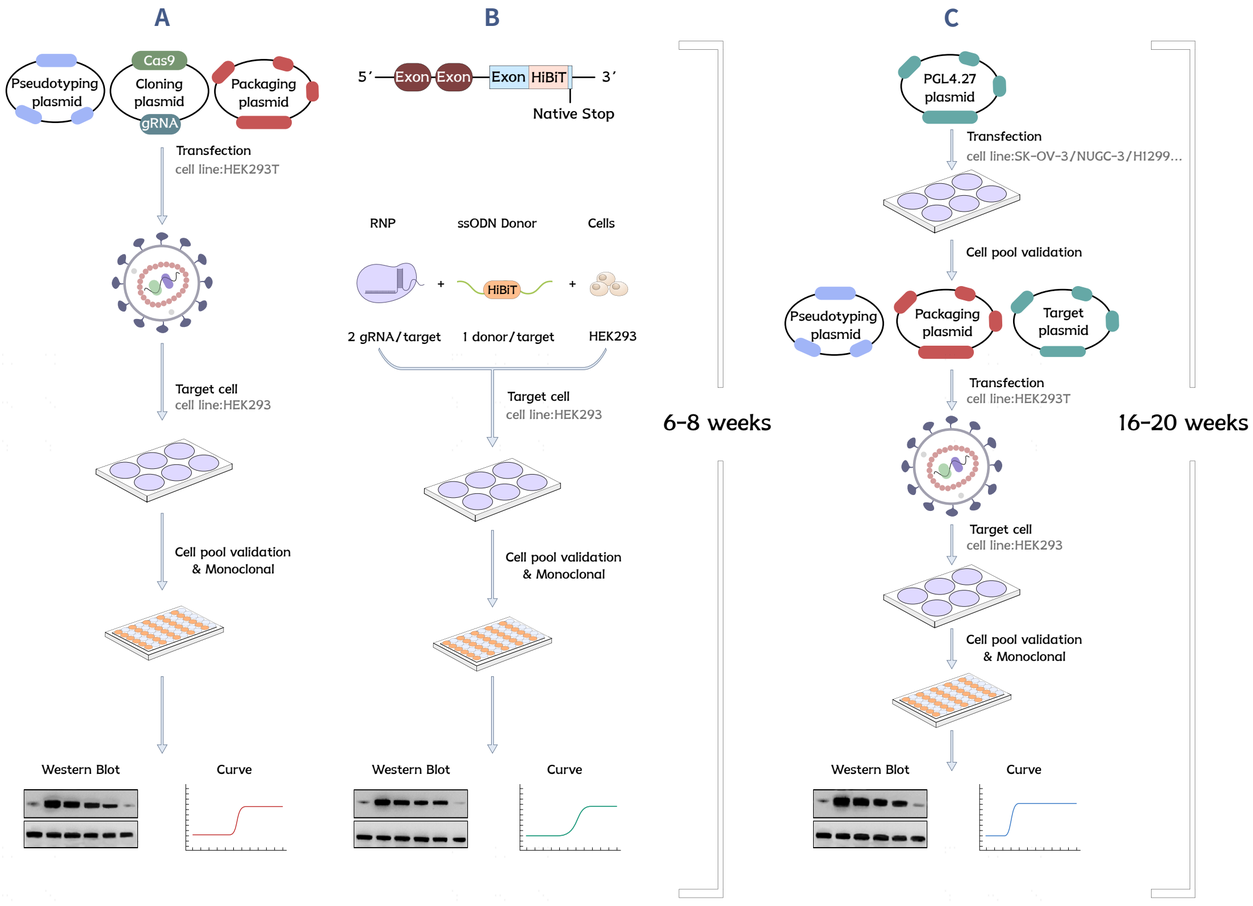

Figure 2. Construction Process of p53 KO, p53 HiBiT & p53RE-Luc2P Cell Lines.

(A) In constructing the p53 KO cell line, the Cas9 plasmid was introduced into HEK 293 cells via lentivirus transfection, followed by puromycin selection and verification of functionality through Western Blot (WB) and proliferation assays.

(B) For the p53 HiBiT cell line, Cas9, donor DNA, and plasmid were electroporated into HEK 293 cells, with subsequent puromycin selection and functional verification using WB and proliferation assays.

(C) The designed plasmid was transiently transfected into target cells. Following puromycin selection, a cell pool was established. The functionality of this pool was confirmed through Western Blot (WB) analysis and proliferation assays. Subsequently, for the construction of the p53 HiBit cell line, the packaging plasmid, vector plasmid, and target plasmid were introduced into the cell pool via lentiviral transfection. Post-puromycin selection, the p53 HiBit cell line's functionality was again verified using WB and proliferation assays. Finally, monoclonal cells were isolated using a single cell per well approach, and their functions were validated through WB and proliferation experiments.

Successful Construction of TP53-KO Cell Line and TP53-P53RE-Luc2P Cell line

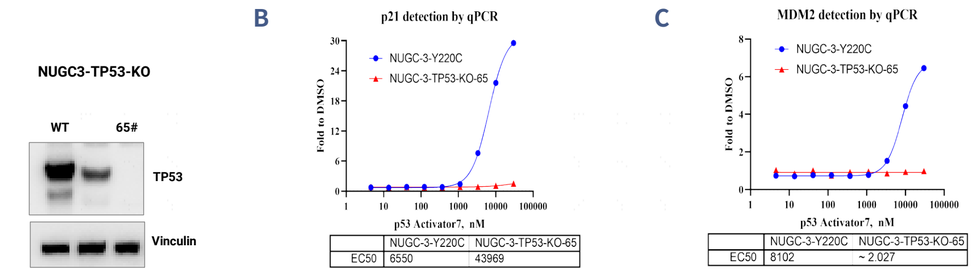

	NUGC-3-Y220C	NUGC-3-TP53-KO-65
EC50	6550	43969

	NUGC-3-Y220C	NUGC-3-TP53-KO-65
EC50	8102	~ 2.027

Figure 6. Construction and Characterization of the NUGC-3-TP53-KO Cell Line.

(A) Western blot (WB) analysis demonstrating TP53 protein levels, with Vinculin serving as a loading control. The absence of a TP53 band in the TP53-knockout (KO) cells (third lane) compared to the wild-type (first lane) indicates effective knockout.

(B) Quantitative PCR (qPCR) results showing the expression of the P21 gene in NUGC-3-Y220C and NUGC-3-TP53-KO cell lines. The graph indicates a relative expression level.

(C) qPCR results for the MDM2 gene expression in NUGC-3-Y220C and NUGC-3-TP53-KO cell lines, with the graph illustrating relative gene expression levels.

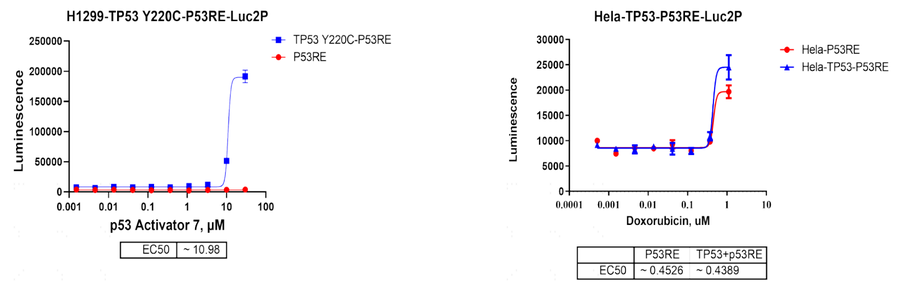

	P53RE	TP53+p53RE
EC50	~ 0.4526	~ 0.4389

Figure 7. The H1299-TP53 Y220C-P53RE-Luc2P & Hela-TP53 Y220C-P53RE-Luc2P cell line was succeessfully constructed using reporter assay.

Quantification of P53 Downstream Antioxidant Factor GSH

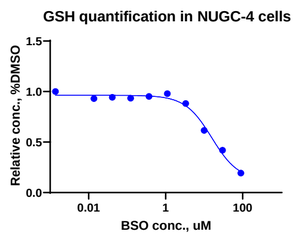

	GSH
IC50	15.84

Figure 8. GSH Depletion in NUGC-4 Cells by treatment with l -buthionine-(S,R)-sulfoximine (BSO). The quantification of GSH, an important antioxidant and a key molecule in cellular redox homeostasis, is essential for understanding the cellular oxidative stress response, particularly in the context of p53 activation. p53 can induce the expression of several redox-related genes, influencing the cellular response to oxidative stress. Thus, monitoring GSH levels post-BSO treatment can provide insights into the downstream effects of p53 activation and the overall redox balance within the cells.

CDX Models with P53

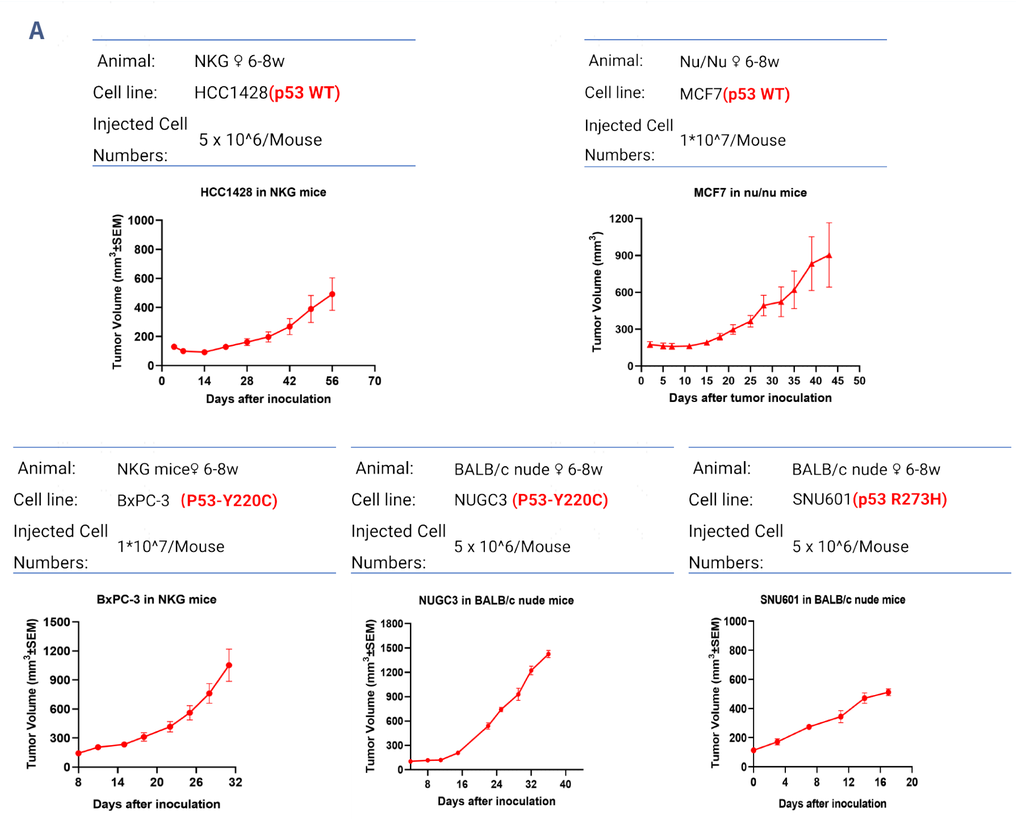

Figure 9. Comparative Tumor Growth Curves in Mouse Models with Varied p53 Status.

Tumor volume progression in mice inoculated with cancer cell lines exhibiting different p53 genetic statuses.

(A) HCC1428 cells with wild-type p53 (p53 WT) in NKG mice show steady tumor growth over 70 days. MCF7 cells with wild-type p53 in nu/nu mice demonstrate a similar increase in tumor volume, peaking at around 50 days post-inoculation.

(B) BxPC-3 cells harboring the p53-Y220C mutation in NKG mice exhibit rapid tumor volume increase within 32 days. (Bottom Right) Comparative growth of NUGC3 cells in BALB/c nude mice with p53-R273H mutation and SNU601 cells with wild-type p53, both showing a marked increase in tumor volume, albeit at different rates, over the monitored period. These growth profiles suggest a correlation between p53 status and tumor progression dynamics in vivo.

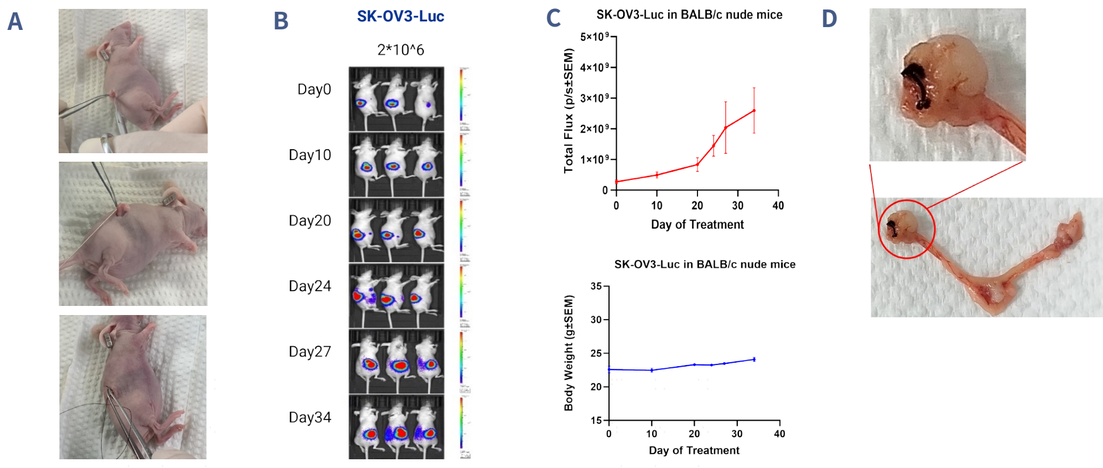

Figure 10. Orthotopic Ovarian Cancer Model Evaluation Using SK-OV3-Luc Mice. The series of images demonstrates the establishment and progression of an ovarian cancer model. (A) The top panel provides a stepwise illustration of the orthotopic implantation of SKOV3-luc cells into the ovarian bursa, demonstrating the initial procedure for establishing the cancer model. (B) The in vivo imaging tracks the development of tumors via bioluminescence in SK-OV3-luciferase expressing cells, with the corresponding tumor growth and body weight curve shown on the right (C). After the endpoint, the reproductive tracts were removed and photographed (D) to provide a direct visualization of the tumor burden, with the primary tumor mass clearly circled.

Conclusions

In conclusion, the comprehensive capabilities of our platform have been instrumental in advancing p53 research, as demonstrated by the successful construction of p53 knockout and p53 HiBiT cell lines, along with the p53 Response Element (p53RE)-Luc2P reporter lines, which have been pivotal in the functional analysis of p53's role in the DNA Damage Response (DDR) pathway. Our platform encompasses a wide range of assays, including protein purification, biochemical assays, cellular phenotypic assays, and in vivo pharmacology studies. The use of luminescent reporter assays facilitated the functional validation of p53 interactions, and the quantification of the downstream antioxidant factor GSH emphasized the impact of p53 on cellular redox homeostasis. Our in vivo models provided further insights into the dynamics of tumor progression, reinforcing the translational relevance of our research platform. Overall, our integrated approach has enabled us to dissect the complexities of p53 biology and contribute significantly to the identification of therapeutic strategies targeting the DDR pathway.

References

[1] Bauer MR, et al. A structure-guided molecular chaperone approach for restoring the transcriptional activity of the p53 cancer mutant Y220C [published correction appears in Future Med Chem. 2021 Mar;13(6):593-594] Future Med Chem. 2019;11(19):2491-2504.

[2] Hu J, Cao J, Topatana W, et al. Targeting mutant p53 for cancer therapy: direct and indirect strategies[J].